Influence of Molecular Structure on the Rate of Intersystem Crossing in Flexible Biradicals

Yuri P. Tsentalovich,* Olga B. Morozova, Nikolai I. Avdievich,† Gennady S. Ananchenko, Alexandra V. Yurkovskaya, Jonathan D. Ball,† and Malcolm D. E. Forbes†

International Tomography Center, Institutskaya 3a, 630090, Novosibirsk-90, Russia, and Venable and Kenan Laboratories, Department of Chemistry, CB#3290, University of North Carolina, Chapel Hill, North Carolina 27599

Received: August 20, 1997[⊗]

Laser flash photolysis (LFP), low-field chemically induced dynamic nuclear polarization (CIDNP), and time-resolved electron paramagnetic resonance (TREPR) techniques have been used for the comparative study of magnetic field and spin effects in acyl−ketyl and bis(ketyl)biradicals formed during the photolysis of 2-hydroxy-2,12-dimethylcyclododecanone (1-OH) and 2,12-dihydroxy-2,12-dimethylcyclododecanone (2-OH), respectively. The short biradical lifetime, the small magnetic field effect (MFE) on a biradical lifetime, and the low intensity of spin-correlated radical pair (SCRP) polarization observed during the photolysis of 1-OH indicate that the main channel of intersystem crossing in acyl−ketyl biradical is spin−orbit coupling (SOC). For bis(ketyl) biradicals observed during the photolysis of 2-OH, SOC is of minor importance, and both MFE and SCRP polarization are much larger. It is shown that the presence of significant SOC in biradicals can result in an increase of the CIDNP intensity at low magnetic fields. Calculations of biradical evolution, based on the numerical solution of the stochastic Liouville equation (SLE), were carried out by taking into account (1) the molecular dynamics of the polymethylene chain linking the radical centers, (2) the distance-dependent exchange interaction, (3) the chemical reactions of the biradical, (4) the spin relaxation processes, and (5) state-to-state transitions caused by hyperfine interaction and SOC. A common set of parameters was found which allows quantitative description of the field dependence of the biradical lifetime, the CIDNP field dependence, and the TREPR spectra and kinetics.

Introduction

Flexible biradicals generated during the photolysis of cyclic aliphatic ketones have been widely used as model systems for the investigation of the interradical interactions in geminate processes.[1] Since the radical centers of the biradical are linked by a carbon chain, no diffusive separation can occur and as a result the geminate processes in biradicals are prolonged in time in comparison with those for typical radical pairs in solution. Under these circumstances, modern time-resolved spectroscopic methods can be successfully applied to study the time evolution of geminate radical pair processes. Another consequence of radical centers being linked together is that the average value of the exchange integral (J) is much higher than in radical pairs and depends strongly on the biradical chain length and dynamics.[2−6]

When biradicals are generated from the excited triplet state of a parent molecule, two processes determine their lifetime: intersystem crossing (ISC) from the nonreactive triplet state to the ground singlet state and conformational movement of the polymethylene chain linking the radical centers. The latter modulates the interradical distance, varying the biradical from the "extended state", where the radical centers are far apart, to the "closed state", where chemical reaction can occur. It has been shown both theoretically and experimentally[5,7] that at room temperature in nonviscous solutions, the biradical molecular dynamics are faster than the spin dynamics. Consequently, biradical lifetime in these systems is determined by the rate of triplet−singlet evolution. There are three main channels which cause triplet−singlet transitions in biradicals: electron spin relaxation, hyperfine interaction, and spin−orbit coupling (SOC).

In previous experiments in our laboratories, we studied acyl−alkyl biradicals generated by UV laser irradiation of cyclic aliphatic ketones. It is well established that the presence of the carbonyl group enlarges the spin−orbit interaction.[3a,7,8] Indeed, the small magnetic field effect (MFE) on biradical lifetime[3a,7a] and the small intensity of CIDNP in high magnetic fields, compared to that theoretically predicted,[9] indicate that the nuclear spin-independent transitions due to SOC are the main channel for intersystem crossing in acyl−alkyl biradicals. However, for ketyl and benzyl biradicals, large MFEs were observed by Tanimoto et al.[10] and Wang and co-workers.[11] These results confirm the dominant role of ISC induced by hyperfine interaction (HFI) in the time evolution of these biradicals.

The aim of the present work is to make a quantitative study of the influence of biradical structure on the relationship between rates of SOC-induced and HFI-induced ISC. For this purpose, two α-substituted cyclic ketones have been synthesized: 2-hydroxy-2,12-dimethylcyclododecanone (1-OH) and 2,12-dihydroxy-2,12-dimethylcyclododecanone (2-OH).[12,13] Upon UV irradiation, both ketones undergo Norrish type I α-cleavage and form triplet acyl−ketyl biradicals. It was recently shown that $(CH_3)_2(OH)C\dot{C}O$ monoradicals undergo thermal decarbonylation at room temperature with a rate constant of about 10^8 s^{-1},[14] whereas the decarbonylation rate constant of the pivaloyl radical is about 10^6 s^{-1}.[15] Thus, one can expect that the acyl−ketyl biradicals generated during the irradiation of 2-OH will also undergo fast decarbonylation and will form symmetric bis(ketyl) biradicals (Scheme 1). The influence of the spin−orbit coupling

* Author to whom correspondence should be addressed.
† University of North Carolina.
⊗ Abstract published in *Advance ACS Abstracts,* November 1, 1997.

S1089-5639(97)02717-5 CCC: $14.00

SCHEME 1: Formation of Magnetic and Spin Effects in Biradicals during the Photolysis of 1-OH and 2-OH

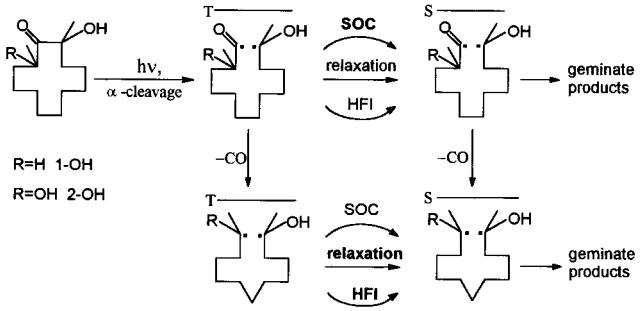

in these biradicals should be less important than in the primary acyl−ketyl biradicals.

In this work, we have applied complementary methods for comparative study of these two types of biradicals: TREPR, low-field CIDNP, and laser flash photolysis (LFP). TREPR was used for the identification of intermediates formed under laser irradiation and for the measurements of the spectra and kinetics of electron polarization (CIDEP). The CIDNP method was applied to the comparative study of nuclear polarization intensities in the reaction products formed in these systems and their magnetic field dependencies. Finally, LFP experiments provided the information about the magnetic field effect on biradical lifetimes.

Experimental Section

Reagents. Synthesis of compounds 1-OH and 2-OH was accomplished as described in our previous publications.[12,13] Solvents methanol (Merck) and deuterated methanol (Isotop) were used as received.

TREPR Measurements. Our TREPR apparatus has been described elsewhere.[16] Additionally, special means were undertaken in order to avoid the distortion of the signal kinetics due to a low frequency cutoff in the detection part of our setup.[17] The measurements were performed on a JEOL USA (Peabody, MA) JES−RE1X X-band (9.46 GHz) EPR spectrometer. TREPR spectra were obtained by applying the output of the spectrometer amplifier to the input of a Stanford Research Systems (SRS) boxcar signal averager SR 250 (Sunnyvale, CA). For the kinetic measurements a LeCroy 9400B (Spring Valley, NY) transient digitizer was used. For UV light excitation we used a Lambda Physik LPX-l00i excimer laser operating at 308 nm (XeCl).

LFP Measurements. A detailed description of our LFP setup was given earlier.[18] The sample solutions were irradiated in a flowing quartz cell with 2 × 10 mm inside dimensions by pulses of a home-made excimer laser (308 nm, pulse energy up to 150 mJ). The monitoring system consisted of a 150 W short-arc Xe lamp DKsSh-150 equipped with a home-made pulse (pulse duration 2 ms), two synchronously operating home-made monochromators, a set of spherical lenses, a shutter, a Hamamatsu R955 photomultiplier, and a digital oscilloscope LeCroy 9310A. The cell was placed inside a home-made magnet. The magnetic field (up to 360 mT) was controlled by a Sh1-8 magnetometer.

CIDNP Measurements. Setup for low-field CIDNP measurements has been described elsewhere.[19] The solutions were irradiated inside a home-made magnet by pulses of a Lambda Physik COMPEX-110 excimer laser (308 nm) and then were transferred by a flow system into the probe of a MSL-300 (Bruker) NMR spectrometer. The transfer time was about 2 s.

For comparative study of the polarization and magnetic field effects in the photolysis of 1-OH and 2-OH, the solutions of these two compounds were prepared with approximately equal optical densities at 308 nm in all types of experiments. The typical optical densities at 308 nm were 0.04 in TREPR experiments (optical pathway 0.5 mm), 0.07 in LFP experiments (2 mm), and 0.5 in CIDNP experiments (10 mm). Prior to irradiation, all samples in all types of experiments were purged with argon or with nitrogen for at least 30 min.

Theory

The theoretical approach we use for the modeling of the biradical evolution has been described in detail in our previous publications,[13,20] and therefore we report here only its general framework and some modifications made in this work. Our calculations were based on the de Kanter[5] approach for the description of the CIDNP field dependencies in the geminate recombination of biradicals, which involves the numerical solution of the stochastic Liouville equation (SLE):

$$\frac{\partial\rho(t)}{\partial t} = -\mathrm{i}\hat{L}\rho(t) + \hat{R}\rho(t) + \hat{W}\rho(t) + \hat{K}\rho(t) \qquad (1)$$

Here $\hat{L}$ is the Liouville operator which is associated with the spin Hamiltonian $\hat{H}$ in accordance with the equation $\hat{L}\rho(t) = \hat{H}\rho(t) - \rho(t)\hat{H}$, $\hat{R}$ is the relaxation matrix, $\hat{W}$ characterizes the dynamic behavior of the polymethylene chain, and $\hat{K}$ represents the chemical reactions of the biradicals.

The spin Hamiltonian includes the Zeeman interaction of the electrons having g-factors g_1 and g_2 with the external magnetic field B_0, electron−nuclear hyperfine interaction with the hyperfine coupling constants A_i and A_j, and the exchange interaction between the unpaired electrons $J(r)$:

$$\hat{H} = \beta_e B_0(g_1\hat{S}_{1z} + g_2\hat{S}_{2z}) + \sum_i \hbar A_i \hat{S}_{1z}\hat{I}_z + \sum_i \hbar A_i(\hat{S}_{1x}\hat{I}_x + \hat{S}_{1y}\hat{I}_y) - \hbar J(r)(1/2 + 2\hat{S}_1\hat{S}_2) \qquad (2)$$

The exchange interaction is assumed to be decaying exponentially with the biradical end-to-end distance r:

$$J(r) = J_0 \mathrm{e}^{-\alpha r} \qquad (3)$$

For a description of the conformational motion of the polymethylene chain of the biradical, an end-to-end distance distribution function[5] was calculated and then divided into $m = 200$ segments of equal area. Transitions between neighboring segments i and k were described by the $\hat{\mathbf{W}}$ matrix:

$$W_{ik} = W_{ki} = \frac{D}{(r_i - r_k)^2} \qquad (4)$$

where D is the effective diffusion coefficient and r_i is an average end-to-end distance for segment i.

The $\hat{R}$ matrix includes the elements determined by two mechanisms of spin relaxation: uncorrelated relaxation, characterized by fluctuations of the local magnetic fields $\langle|B_i|^2\rangle$ and correlation time τ_u, and correlated interactions, characterized by rotational correlation time τ_c (dipole−dipole relaxation).[5,11]

The $\hat{\mathbf{K}}$ matrix describes the chemical reactions of the biradicals: (a) recombination of biradicals from the singlet state at the smallest end-to-end distance $r = r_d$ with the rate constant k_r, (b) "scavenging" reactions, removing biradicals from geminate recombination, disregarding their spin state and end-to-end distance (decarbonylation, reactions with radical scavengers or solvent impurities, and so on), and (c) biradical decay due to spin−orbit coupling. The latter is taken into account as

recombination from triplet substates T_i (T_0, T_+, T_-) at $r = r_d$ with rate constant k_{soc}.[8]

Taking into account the difference in rates of decarbonylation for the two types of primary acyl−ketyl biradicals (see below), we assume that the photolysis of the starting ketones produces only one type of biradical (acyl−ketyl biradicals for 1-OH and bis-ketyl ones for 2-OH), which are formed with equally populated triplet sublevels at $r = r_d$.

Unfortunately, this approach does not allow calculation of low-field effects taking into account all magnetic nuclei because the dimensions of the matrices become too large. For this reason, our calculations used two different approaches: a low-field model (LFM) and a high-field approximation (HFA). In HFA, only the secular part of the HFI ($\sum_i A_i \hat{S}_{1z}\hat{I}_{iz} - \sum_j A_j \hat{S}_{2z}\hat{I}_{jz}$), with all magnetic nuclei was taken into account. In this case, four wave functions were used as a basis: S, T_0, T_+, and T_-; hence, the spin density matrix consisted of 16 elements. In LFM, all electron−nuclear transitions were taken into account, but the magnetic interactions of the electron with all nuclei were replaced by interaction with only one nucleus with the effective HFI constant A_{eff}. The direct products of the electron and nuclear spin functions were used as a basis (Sα, $T_0\alpha$, $T_+\alpha$, $T_-\alpha$, Sβ, $T_0\beta$, $T_+\beta$, $T_-\beta$). In this work, LFM was used for the description of the CIDNP field dependence (magnetic field 0−0.1 T) and the field dependence of the biradical lifetimes (0−0.36 T). HFA was applied for the simulation of TREPR spectra and kinetics (0.33 T) and for the description of the high-field part of the field dependence of the biradical lifetime (0.1−0.36 T).

For the calculation the CIDNP magneticfield dependence, the stochastic Liouville equation was solved for the Laplace transformation of the spin density matrix $\rho(s) = \int_0^\infty \rho(t)e^{-st}\,dt$, which yields the stationary in *s*-domain equation for the spin density matrix:[5]

$$s\rho(s) + i\hat{L}\rho(s) - \hat{R}\rho(s) - \hat{W}\rho(s) - \hat{K}\rho(s) = \rho^0 \qquad (5)$$

where $\rho^0 = \rho(t = 0)$

The CIDNP amplitude was calculated according to eq 6:

$$P = k_r[\rho_{S\alpha S\alpha}(s)|_{r=r_d} - \rho_{S\beta S\beta}(s)|_{r=r_d}] + k_{soc}\sum_i [\rho_{T_i\alpha T_i\alpha}(s)|_{r=r_d} - \rho_{T_i\beta T_i\beta}(s)|_{r=r_d}] \qquad (6)$$

To calculate the *biradical lifetime* τ we used the dependence of the geminate product yield Pr on the value of the parameter *s*, which corresponds to the scavenging rate constant:

$$\tau = \frac{Pr(0) - Pr(s)}{sPr(s)} \qquad (7)$$

with

$$Pr(s) = k_r[\rho_{S\alpha S\alpha}(s)|_{r=r_d} + \rho_{S\beta S\beta}(s)|_{r=r_d}] + k_{soc}\sum_i [\rho_{T_i\alpha T_i\alpha}(s)|_{r=r_d} + \rho_{T_i\beta T_i\beta}(s)|_{r=r_d}] \qquad (8)$$

Since at $s = 0$ all the biradicals recombine to give geminate product, $Pr(0) = 1$ and

$$\tau = \frac{1 - Pr(s)}{sPr(s)} \qquad (9)$$

The polarized *TREPR spectra* were simulated according to the following procedure. First, the Hamiltonian of the system was modified for the case of the interaction of the electron spin with the microwave field as described earlier:[21]

$$\hat{H}' = \hat{H} + \hat{H}_1(t) \qquad (10)$$

where $\hat{H}$ is described by eq 2 and

$$\hat{H}_1(t) = \beta_e\hbar^{-1}B_1[(g_1\hat{S}_{1x} + g_2\hat{S}_{2x})\cos\omega t + (g_1\hat{S}_{1y} + g_2\hat{S}_{2y})\sin\omega t)] \qquad (11)$$

In eq 11 B_1 is the amplitude of microwave field and ω is its frequency.

The time dependence of the Hamiltonian was excluded using the transformation to a rotating frame of reference (RFR) by means of a rotation operator $\hat{M}$:

$$\hat{M} = e^{-i\omega\hat{F}_z t}, \quad \hat{F}_z = \hat{S}_{1z} + \hat{S}_{2z} + \hat{I}_z \qquad (12)$$

Application of the $\hat{M}$ operator to $\hat{H}_1$

$$\hat{H}_{1r} = e^{i\omega\hat{F}_z t}\hat{H}_1 e^{-i\omega\hat{F}_z t} \qquad (13)$$

makes the latter time-independent:

$$\hat{H}_1(t) = \beta_e\hbar^{-1}B_1(g_1\hat{S}_{1x} + g_2\hat{S}_{2x}) \qquad (14)$$

The operators $\hat{L}$, $\hat{R}$, $\hat{W}$, $\hat{K}$ in eq 1 are axially symmetric and stay unchanged under transformation to RFR. As in case of the CIDNP calculation, the SLE (1) was solved using the Laplace transformation of the spin density matrix. To obtain the TREPR spectrum, we calculated $\langle\hat{S}_y\rangle$ according to eq 15 as a function of B_0,

$$\langle\hat{S}_y\rangle = \sum_j\langle\hat{S}_y\rangle_j = \sum_j \mathrm{Tr}(\hat{S}_y\rho_j) \qquad (15)$$

where *j* denotes the number of a particular slice of the end-to-end distribution function.

To calculate the *time dependencies of TREPR line intensities* at certain magnetic fields B_0, we applied the approach for calculating $\rho(t)$ described in our previous papers.[13,20] This approach is based on the numerical solution of the stochastic Liouville equation for the Fourier transform $\tilde{\rho}(\omega)$ of the spin density matrix. Substitution of the Fourier transform $\tilde{\rho}(\omega) = \int_0^\infty \rho(t)e^{-i\omega t}\,dt$ into eq 1 gives the stationary equation for $\tilde{\rho}(\omega)$, which could be solved numerically as in the case of using the Laplace transformation. The Fourier reconstruction of $\tilde{\rho}(\omega)$ yields a time-dependent density matrix $\rho(t)$, which allows to obtain the TREPR kinetics in accordance with eq 15. During the calculations the number of harmonics in the Fourier series was equal 1000 with the highest frequency $\omega_0 = 2\pi/T$, where *T* was equal to 5 μs.

Results

1. TREPR Results. Figure 1 shows experimental and simulated TREPR spectra obtained at room temperature during the photolysis of 2-OH in methanol at 0.8 and 2.0 μs delay times. The simulation parameters will be discussed below. The spectrum obtained at 0.8 μs delay time contains only the spin-correlated radical pair (SCRP) polarization pattern, which is well described in the literature.[22] Simulation of this spectrum unambiguously indicates that the signal carrier is the symmetric bis(ketyl) biradical. During the photolysis of 2-OH, similar spectra were observed even at delay times shorter than 0.1 μs. This confirms that the decarbonylation of the acyl−ketyl

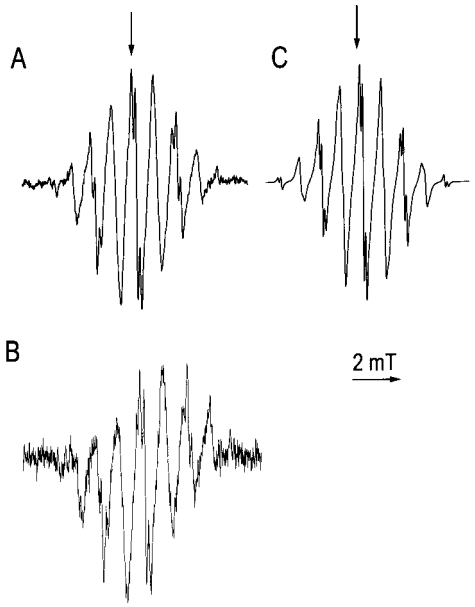

Figure 1. Experimental (A) 0.8 μs and (B) 2.0 μs after the laser pulse and simulated (C) TREPR spectra obtained during the photolysis of 2-OH in methanol at room temperature (for parameters of simulation see Table 1).

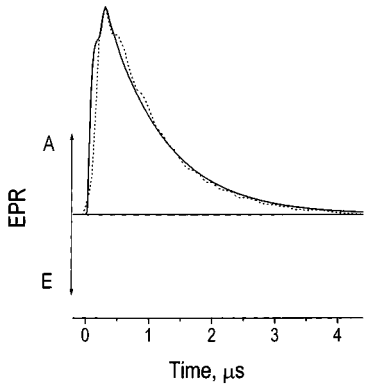

Figure 2. Experimental (dotted lines) and calculated (solid line) kinetics of SCRP polarization (in arbitrary units) of bis(ketyl) biradicals generated during the photolysis of 2-OH. The calculated kinetics is obtained for the EPR transition marked by an arrow in Figure 1. For parameters of calculation see Table 1.

biradicals produced during the photolysis of 2-OH is faster than the time resolution of our experimental setup (ca. 50 ns). It is noteworthy that under similar experimental conditions, the intensity of the bis(ketyl) biradical SCRP spectrum obtained during the photolysis of 2-OH is about an order of magnitude higher than that due to the acyl−ketyl biradical recorded during the photolysis of 1-OH. The spectra obtained at earlier delay times have some admixture of absorptive character, which can be attributed to a contribution from the triplet mechanism, whereas the spectra recorded 2−3 μs (Figure 1B) after the laser pulse show net emissive polarization due to S−T_- mixing which is typically found in short biradicals with negative exchange interactions. The spectra observed at later times also show some uneven intensities relative to the center of the spectrum, (emissive low field lines and absorptive high field lines) which we failed to simulate using high-field approximation, vice infra.

Figure 2 shows experimental and calculated TREPR kinetics (in arbitrary units) obtained for the central line in the spectrum of bis(ketyl) biradicals generated during the photolysis of 2-OH. The transition is marked with an arrow in Figure 1. The shape of the kinetic curves depends only slightly on the laser intensity and the initial concentration of the solutions. We also varied

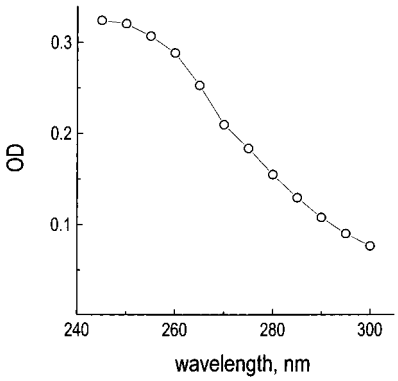

Figure 3. Transient absorption spectrum obtained during the photolysis of 1.2×10^{-2} M solution of 2-OH in methanol 0.1 μs after the laser pulse.

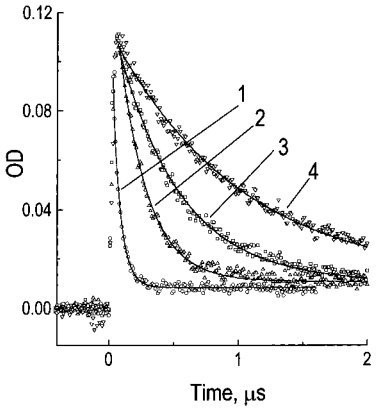

Figure 4. Transient absorption kinetics observed at 270 nm (1) during the photolysis of 1-OH in methanol at zero magnetic field, and during the photolysis of 2-OH in methanol (2) at zero magnetic field, (3) at $B_0 = 90$ mT, and (4) at $B_0 = 300$ mT. Solid lines show the exponential fit.

the microwave field B_1 in the range of 1−50 mW without any noticeable changes in the kinetic behavior.

The TREPR spectrum of the acyl−ketyl biradical obtained during the photolysis of 1-OH will be published elsewhere.[13] The TREPR kinetic curve for these biradicals obtained during the photolysis of 1-OH is similar to the kinetics reported for acyl−alkyl biradicals[16] and decays completely within 300 ns.

2. LFP Results. The transient absorption spectrum obtained 0.1 μs after the flash photolysis of 1.2×10^{-2} M solution of 2-OH in methanol is shown in Figure 3. The same spectrum has been obtained during the photolysis of 1-OH. These spectra are very similar to those of the 2-hydroxy-2-propyl radical[14,23] and correspond to the absorption of ketyl moieties of the acyl−ketyl and bis(ketyl) biradicals. Figure 4 shows the absorption kinetic curves, observed at 270 nm at zero magnetic field, at $B_0 = 90$ mT, and at $B_0 = 300$ mT during the photolysis of 2-OH and at zero magnetic field during the photolysis of 1-OH. The signal from the acyl−ketyl biradical decays with a rate constant $k = (1.5 \pm 0.1) \times 10^7$ s^{-1} at zero magnetic field. Figure 5 shows the magnetic field dependence of the biradical decay rate constants. The rate constant for acyl−ketyl biradical decay depends only slightly on the applied magnetic field while the decay of the bis(ketyl) biradicals is significantly slower ($k = (4.5 \pm 0.3) \times 10^6$ s^{-1} at zero magnetic field) and depends strongly on the magnetic field. At the highest available magnetic field (B_0) of 0.36 T, the biradical lifetime becomes about 5 times longer than that at zero magnetic field. It should be noted that the biradical lifetime magnetic field dependence has not reached saturation at 0.36 T, and at higher magnetic fields one would expect even larger effects.

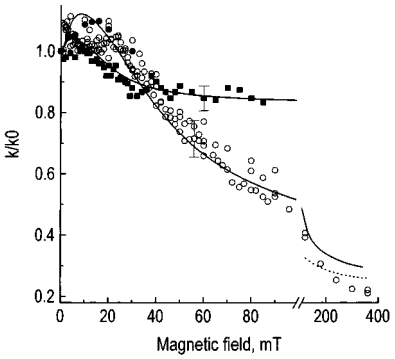

Figure 5. Magnetic field effect on the first order decay rate constant for acyl−ketyl (■) and bis(ketyl) (○) biradicals. Solid lines: model calculations according to the procedure described in the text in frames of LFM. Dotted lines: in frames of HFA, with the parameters listed in Table 1.

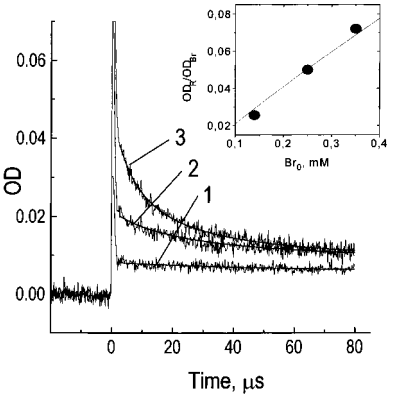

Figure 6. Transient absorption kinetics observed at long time scale at 270 nm in zero magnetic field during the photolysis of 2-OH at different laser output energy: (1) 29 mJ/pulse, (2) 50 mJ/pulse, (3) 70 mJ/pulse. Calculated curves correspond to second-order fit. Insert: the dependence of the ratio of initial adsorptions of bis(ketyl) biradicals and monoradicals on the initial biradical concentration.

In addition to the biradical signal which decays within 1−2 μs under intense laser irradiation, a slowly decaying signal has been also observed (Figure 6). The spectrum of this intermediate is the same as for the biradical; the signal decays according to second-order kinetics, and the initial intensity of this signal depends nonlinearly on the laser power. We have attributed this signal to ketyl monoradicals, formed due to the intermolecular disproportionation of bis(ketyl) biradicals. With long biradical lifetimes, this reaction is expected when the initial biradical concentration is high. It was assumed that the quantum yield of biradicals from the exited triplet state of the parent molecules is equal to unity. For different laser energies the initial biradical concentration in our experimental conditions was varied in the range between 1.5×10^{-4} and 3.5×10^{-4} M. A set of differential equations describing the time dependence of biradical (Br) and monoradical (R) concentrations can be written as

$$\mathrm{dBr}/\mathrm{d}t = -k_1\mathrm{Br} - 2k_2\mathrm{Br}^2 \qquad (16)$$

$$\mathrm{d}R/\mathrm{d}t = -2k_1\mathrm{Br}^2 - 2k_3R^2 \qquad (17)$$

where $k_1 = 4.5 \times 10^6$ s^{-1} is the biradical first-order decay rate constant at zero magnetic field, and k_2 and k_3 are the second-order termination rate constants for bis(ketyl) biradicals and ketyl monoradicals, respectively.

Since the typical monoradical signal lifetime under our experimental conditions is in the order of tens of microseconds,

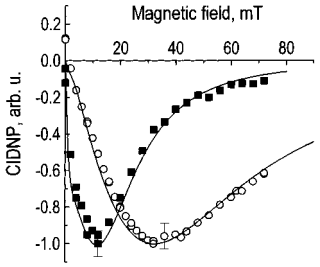

Figure 7. Normalized ^{1}H CIDNP field dependencies for the products of the photolysis of 1-OH (■) and 2-OH (○). Solid lines: model calculations according to the procedure described in the text with the parameters listed in Table 1.

the second term in formula (17) can be neglected for the observation time of a few microseconds after the laser flash. After this simplification, the solution of differential equations (16) and (17) gives the dependence of the initial monoradical concentration R_0 immediately after the biradical decay on the initial biradical concentration Br_0:

$$\frac{R_0}{\mathrm{Br}_0} = 1 - \frac{k_1}{2k_2\mathrm{Br}_0}\ln\left(1 + \frac{2k_2\mathrm{Br}_0}{k_1}\right) \qquad (18)$$

We can assume that the absorption coefficient of the monoradical is half that of the biradical. Hence, the measured ratio of the initial adsorptions of monoradicals and biradicals is $\mathrm{OD_R}/\mathrm{OD_{Br}} = R_0/2\mathrm{Br}_0$. Fitting of eq 18 to the experimental results (Figure 6, insert) gives the rate constant for second order biradical termination $2k_2 = (1.9 \pm 0.3) \times 10^9$ M^{-1} s^{-1}.

3. Low-Field CIDNP. The magnetic field dependencies of CIDNP signals obtained during the photolysis of 2×10^{-2} M solutions of 1-OH and 2-OH in CD_3OD are shown in Figure 7. The shapes of CIDNP magnetic field dependencies, obtained during the photolysis of 1-OH, were the same for all reaction products. The curves obtained for the products of primary acyl−ketyl and of secondary bis(ketyl) biradicals during the photolysis of 2-OH were different. Figure 7 shows the CIDNP in the products of the secondary biradical. The low-field CIDNP spectra and a detailed study of CIDNP formation in consecutive biradicals will be published elsewhere.[24] It should be noted that the overall CIDNP intensity observed during the photolysis of 1-OH was higher than that observed during the photolysis of 2-OH.

Discussion

As stated above, there are three channels of the intersystem crossing of triplet biradical to the reactive singlet state: hyperfine interaction, electron spin relaxation, and spin−orbit coupling. At magnetic fields below 100 mT, hyperfine interaction is the main channel leading to the formation of magnetic and spin effects; however, at larger magnetic fields, the dependence of the rate of electron relaxation on magnetic field is expected. Since the spin−orbit interaction is a nuclear spin independent channel of the intersystem crossing, the presence of noticeable SOC usually results in decreasing of magnetic and spin effects.

The SOC in acyl−ketyl biradical can be considered as an additional element of the relaxation matrix, which causes fast electron transitions in the acyl moiety of the biradical and, subsequently, mixes triplet and singlet sublevels of the biradical. However, de Kanter and Kaptein[8] have shown that the influence of SOC on the biradical reactivity strongly depends on the mutual orientation of the biradical moieties at the closest interradical distance. Hence, SOC effect can be considered as the biradical reaction directly from the triplet state at the contact

TABLE 1: Set of Parameters Common for All Calculations

parameters of calculations	biradical		
	acyl−ketyl		bis(ketyl)
k_{soc}, s^{-1}	2.2×10^9		1.3×10^8
J_0, mT	-0.7×10^9		-1.3×10^9
α, $Å^{-1}$		2.14	
D, cm^2/s		2×10^{-5}	
G, s^{-2}		8×10^{16}	
τ_u, s		10^{-12}	
τ_c, s		8×10^{-11}	
k_r, s^{-1}		10^{11}	

radius. In our paper, we follow this approach (see Theory section). It can be shown that for the fast conformational motion of the biradical, these two approaches are equivalent and give the same result in most cases.

The results obtained in this work unambiguously show that the main channel of ISC and the rate-determining step of acyl−ketyl biradical decay is the spin−orbit interaction. The biradical decay measured in LFP experiments is almost field independent (the magnetic field effect on the biradical lifetime is about 15%). Uncorrelated electron relaxation, caused by dipole−dipole interaction of an electron with the magnetic nuclei, mixes singlet and triplet states of biradical and can also lead to the same result. However, the observed biradical lifetime (67 ns at zero magnetic field) is much shorter than the typical T_1 relaxation times of the corresponding ketyl monoradicals.[25] On the contrary, bis(ketyl) biradicals show a much longer lifetime, which is strongly field dependent (Figure 5). The increase of biradical lifetime in region 30−100 mT can be explained in terms of the increase of the energy gap between S and T_+, T_- states, which results in decrease of HFI-induced part of k_{isc}. At higher magnetic fields (100−360 mT), the field dependence of electron spin relaxation, caused by dipole−dipole interaction of unpaired electrons, should be also taken into account. Thus, one can conclude that for bis(ketyl) biradicals the spin−orbit interaction does not play a significant role, and the main channels of intersystem crossing are hyperfine interaction and electron relaxation.

The kinetics and the relative amplitudes of TREPR spectra obtained during the photolysis of 1-OH and 2-OH confirm these conclusions. As mentioned above, the time scales of TREPR kinetics obtained for these two systems are substantially different. The EPR signal of the acyl−ketyl biradical completely disappears within 300 ns. For this case fast spin-independent SOC seems to be a reasonable mechanism of intersystem crossing. TREPR kinetics obtained during the photolysis of 2-OH are much slower (Figure 2). In bis(ketyl) biradicals where the spin−orbit interaction is not important, the time scale of polarization evolution is completely determined by the rate constants of decays of T_+ and T_- sublevels. Simulation using the high-field SLE model with reasonable relaxation rates (see Table 1) describes the kinetic behavior of the central line very well. The initial rise of the EPR signal is about 200 ns and can be explained by an effect of the spin−spin T_2 relaxation and an apparatus function of our spectrometer which is mostly determined by the Q-factor of the X-band cavity resonator. Kinetic curves measured for other TREPR spectral lines have different decay rates. We failed to simulate all of them for the reasons which are discussed below.

An interesting feature of the TREPR spectra shown in Figure 1 is the alternating line-width pattern, recently described in the literature for SCRPs.[26] This effect has been observed for different symmetric biradicals and explained by the influence of relaxation due to the modulation of exchange interaction J. It is interesting that previously this effect has been observed at room temperature and above for long-chain (21 carbon atoms) (bis)alkyl biradicals which have more effective J-modulation relaxation compared with shorter biradicals.[26a] TREPR spectrum of C_{11} bis(ketyl) biradical also revealed the line-width alternating pattern. Simulation shown in Figure 1C adequately depicts this effect.

Another noteworthy feature observed in TREPR spectra of bis(ketyl) biradical at 2.0 μs delay time is the distortion of the purely symmetric SCRP structure (see Figure 1A) due to the appearance of an E/A pattern in the spectrum. The spectrum shown in Figure 1B has a total integral emissive polarization. Such a distortion can be explained by the presence of S−T_- and S−T_+ transitions in biradicals which were not taken into account in the HFA SLE model. It is well-known that S−T_- transitions are more effective for the low-field part of the spectra while S−T_+ transitions are dominant for the high-field side. The emissive character of the spectra can be accounted for due to the different rates of S−T_+ and S−T_- transitions in the biradical: since the exchange integral is negative, S−T_- transitions go faster, and therefore at longer times the population of T_+ level becomes larger than that of T_- level. The same effects can lead to different kinetic rates for different lines in TREPR spectra of 2-OH biradicals, as mentioned above. S−T_- transitions lead to the appearance of an emissive pattern which is more intense in the low-field part of the spectra. Together with the decay of symmetric SCRP polarization it can appear in TREPR spectrum as an increase in decay rates for low-field absorptive lines and decrease in decay rates for low-field emissive lines. S−T_+ transitions work in an opposite way for the high-field spectral side, decreasing relative decay rates for absorptive and increasing them for emissive high-field lines. Thus, the kinetics of the central line, shown in Figure 2, are less influenced by this effect. The HFA cannot reproduce this effect since it does not take into account S−$T_\pm$ mixing. To check this hypothesis, collection of TREPR spectra and their kinetics at different magnetic fields can be very useful. Such an investigation is currently underway in one of our labs, and a detailed analysis of this matter is beyond the scope of the present paper.

Additional evidence for the different sources of intersystem crossing in acyl−ketyl and bis(ketyl) biradical is provided by the amplitudes of SCRP polarization. When SOC does not play a significant role, the intensity of SCRP polarization can reach a higher level. This is clearly observed during the photolysis of 2-OH. Our setup does not yet allow for absolute measurement of polarization amplitudes, but qualitatively the intensity of the polarization of bis(ketyl) biradicals is about an order of magnitude stronger than that observed in acyl−ketyl biradicals. In acyl−ketyl biradicals, generated during the photolysis of 1-OH, the spin−orbit interaction induces fast nuclear spin-independent triplet−singlet transitions. Thus, the time evolution of the signal becomes much shorter, and the intensity of CIDEP significantly decreases.

At first, the results of CIDNP measurements appear to contradict the results of the LFP and CIDEP experiments: the nuclear polarization of the products of 1-OH photolysis is about twice as large as the polarization of 2-OH photolysis products. For an explanation of this discrepancy, one should consider the kinetics of CIDNP formation in a low magnetic field. Let the biradicals be formed with equal populations of the three triplet states. The formation of CIDNP effects will be controlled by the rates of S−T_- transitions, which occur according to the rule $T_-\alpha \rightarrow S\beta$ (α and β denote the projections of nuclear spin), and of S−T_+ transitions ($T_+\beta \rightarrow S\alpha$). Since the exchange integral $\langle J \rangle$ in biradicals is negative, in a magnetic field $B_0 \sim$

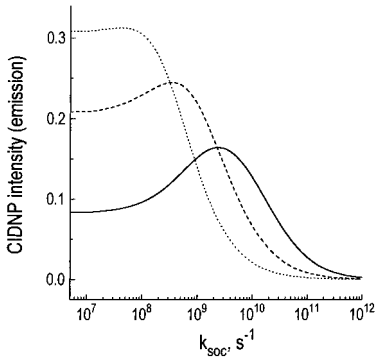

Figure 8. Calculated CIDNP amplitude dependence on the rate constant of spin−orbit coupling at the magnetic field 20 mT for 1,11-biradical for HFI constants 1.5 mT (dotted line), 3 mT (dashed line), and 6 mT (solid line). Other parameters are listed in Table 1 for bis-(ketyl) biradical.

$2|\langle J\rangle|/g_e\beta_e$, the S−T$_-$ transitions become most efficient leading to the formation of an intense emissive nuclear polarization. The S−T$_-$ transitions are followed by S−T$_+$ ones, which form nuclear polarization of an opposite sign, and diminish the observed CIDNP effects. Thus, when electron relaxation and spin−orbit interaction are negligible, the kinetics of CIDNP formation should have an extremum with its position mainly determined by the rate of S−T$_-$ transitions; then the CIDNP decays with a rate determined by S−T$_+$ transitions. The SOC-induced transitions take place without a nuclear spin flip and could "cut off" the slow S−T$_+$ transitions. As a result, the observed nuclear polarization in diamagnetic products will increase. Electron relaxation also mixes triplet and singlet states of the biradical, and the intensity of the observed CIDNP is therefore a rather complicated function of HFI, SOC, and relaxation induced transition rates. Figure 8 shows numerical calculations of the influence of the rate of SOC-induced transitions on the CIDNP intensity for different values of the hyperfine coupling constant (for a description of the theoretical model see Theory). When the hyperfine coupling constant is small (1.5 mT), the main channel of biradical decay from the T$_+$ state in absence of SOC is electron spin relaxation. Thus, the kinetic curve for nuclear polarization, as well as the dependence of CIDNP on the rate of SOC-induced transitions, is monotonous (Figure 8, dotted line). For a larger hyperfine coupling constant (3 and 6 mT) the S−T$_+$ transitions become more important, and the curve passes through the maximum (Figure 8, dashed and solid lines).

We have performed model calculations for the quantitative separation of contributions from spin-dependent and spin-independent processes to ISC, as well as for verifying the values of parameters of intra- and interradical interactions. The parameters used in the calculations are given in Table 1 and were chosen in order to fit the following experimental data: (1) the CIDNP field dependencies for the products of the photolysis of 1-OH and 2-OH; (2) the absolute values of the lifetimes of acyl−ketyl and bis(ketyl) biradicals; (3) the dependencies of decay rate constants on the external magnetic field for acyl−ketyl and bis(ketyl) biradicals; (4) the TREPR spectrum of bis(ketyl) biradical; and (5) The TREPR kinetics of bis(ketyl) biradical.

The parameters for uncorrelated relaxation $G = {}^1/_2 g_e^2\beta_e^2|B_i|^2$ and τ_u were chosen to give the values of $T_1^{-1} = 4G\tau_u/(1 + \omega^2\tau_u^2)$ approximately the same as for ketyl monoradicals (about 3×10^5 s^{-1}). For calculations using the LFM, the effective HFI constant A_{eff} was a fitting parameter, the best results were obtained with $A_{eff} = 2.2$ mT for acyl−ketyl biradical and $A_{eff} = 3.2$ mT for bis(ketyl) biradical. In the HFA, the values of HFI constants $A_{CH_3} = 1.94$ mT and $A_{CH_2} = 1.68$ mT for the ketyl moiety of the biradical were taken from the literature.[27]

The calculated curves are shown in Figures 1, 2, 5, and 7. An excellent agreement has been obtained for the magnetic field dependencies of CIDNP and of biradical lifetimes, as well as for the simulation of SCRP spectrum shown in Figure 1A. The calculated TREPR kinetics also agree with the experimental data fairly well. However, since in HFA S−T$_-$ and S−T$_+$ transitions are neglected, our calculations could not reproduce either the observed TREPR spectrum at 2.0 μs delay time or the kinetics for low- and high-field TREPR spectral lines.

The values of any of the parameters in Table 1 can be changed within some limits, and the corresponding deviations of the calculated curves from the experimental data can be compensated for by adjustment of the other parameters. Nevertheless, the description of the entire set of experimental data by a common set of parameters strongly restricts the freedom in the parameter's variation.

As one would expect, when fitting CIDNP field dependencies, the most sensitive parameters are the exchange interaction J_0 and the falloff parameter α: an increase of J_0 and/or decrease of α shifts the maximum of the field dependencies to higher magnetic fields. Increasing the effective diffusion coefficient D gave the same result. Reasonable agreement with the experimental data could be achieved with changes in J_0 and D within 50% and in α within 10% of the values listed in Table 1. The value of J_0 for bis(ketyl) radicals (1.3×10^9 mT) turned out to be twice as large as that for acyl−ketyl radicals. The same trend of an increase in the averaged exchange interaction value $\langle J\rangle$ in symmetrical bis(alkyl) biradicals as compared with acyl−alkyl biradicals was marked in the simulations of EPR spectra.[3a] This effect may be connected with the greater overlap of the electron orbitals in symmetrical biradicals or the increasing of the distance of the closest approach for bulky bis(alkyl) biradicals.

The correlation time τ_c was enlarged by approximately an order of magnitude compared to the value used by de Kanter.[5] More than a 30% change in this parameter resulted in a noticeable deviation of the calculated effects from the observed CIDNP field dependencies and MFE, as well as the line widths in the SCRP spectra.

Since SOC is the factor determining the lifetime of acyl−ketyl biradicals, the value $k_{soc} = 2.2 \times 10^9$ s^{-1} could be varied only within 20%. The acceptable range of this parameter for bis(ketyl) biradicals is larger, -5×10^7 to 2×10^8 s^{-1}. As was mentioned above, SOC was taken into account as the reaction from the triplet state in conformations with the minimal interradical distance. The total end-to-end distribution function of the biradical was divided into $m = 200$ segments of equal area. Thus, in the framework of our model, the values k_{soc} depend on the number m. For determination of the contribution of SOC into the observed rate constants of biradical decay, it is reasonable to use the values of k_{soc} normalized by number of segments $k_{soc}' = k_{soc}/m$. This gives $k_{soc}' = 1.1 \times 10^7$ s^{-1} and $k_{soc}' = 6.5 \times 10^5$ s^{-1} for acyl−ketyl and bis(ketyl) biradicals, correspondingly. The value $k_{soc'} = 1.1 \times 10^7$ s^{-1} for acyl−ketyl biradicals coincides surprisingly well with the estimation $k_{soc}' = 1.2 \times 10^7$ s^{-1} made by Closs and Redwine from the measurements of CIDNP intensities for acyl−alkyl biradicals.[9] Presuming that the observed biradical decay rate constant $k_{obs} = k_{soc}' + k$, where k is the rate constant of ISC determined by HFI and relaxation, at zero magnetic field we obtain for acyl-ketyl biradical $k_{obs} = 1.5 \times 10^7$ s^{-1}, $k = 4 \times 10^6$ s^{-1}, and $k_{soc}'/k = 2.75$; for bis-ketyl biradical $k_{obs} = 4.5 \times 10^6$ s^{-1}, $k = 3.85 \times 10^6$ s^{-1}, and $k_{soc}'/k = 0.17$

Conclusions

Three different techniques, TREPR, LFP, and low-field CIDNP, have been applied to study the magnetic field and spin effects in flexible biradicals formed during the photolysis of 1-OH and 2-OH. It has been shown that the main channel of the intersystem crossing in acyl−ketyl biradicals generated during the photolysis of 1-OH is spin−orbit coupling, whereas for bis(ketyl) biradicals the triplet−singlet transitions are governed primarily by hyperfine interaction and relaxation processes (Scheme 1). Model calculations of biradical evolution were carried out. It is important to note that the results obtained using the different experimental techniques, namely the field dependence of biradical lifetime, the CIDNP field dependence, and the SCRP spectra, are fairly well described by a theoretical model with a common set of parameters. In a further submission,[24] we will show that the same set of parameters allows us to reproduce the kinetics of CIDNP at high magnetic fields. It is our belief that the model used describes adequately the main properties of biradicals, and the values of the parameters listed in Table 1 reflect the actual interactions in flexible biradicals.

Acknowledgment. This work was supported by the Russian Foundation for Basic Research (Project No. 96-033-2930), INTAS grant no. 96-1269, and by the National Science Foundation (CHE-9522007).

References and Notes

(1) (a) Jonston, L. J.; Scaiano, J. C. *Chem. Rev.* **1989**, *89*, 521, and references therein. (b) Doubleday, C., Jr; Turro, N. J.; Wang, J.-F. *Acc. Chem. Res.* **1989**, *22*, 199, and references therein. (c) Steiner, U. E.; Wolff, H.-J. In *Photochemistry and Photophysics;* Rabek J. F., Ed.; CRC Press: Boca Raton, FL, 1991, pp 68-82.

(2) (a) Closs, G. L.; Doubleday, C. E. *J. Am. Chem. Soc.* 1973, *89*, 521. (b) Closs, G. L. *Adv. Magn. Reson.* **1974**, *7*, 157.

(3) (a) Closs, G. L.; Forbes, M. D. E.; Piotrowiak, P. *J. Am. Chem. Soc.* **1992**, *114*, 3285. (b) Closs, G. L.; Forbes, M. D. E. *J. Am. Chem. Soc.* **1987**, *109*, 6185. (c) Closs, G. L.; Forbes, M. D. E. *J. Phys. Chem.* **1991**, *95*, 1924.

(4) Yurkovskaya, A. V.; Galimov, R. R.; Obynochny, A. A.; Salikhov, K. M.; Sagdeev, R. Z. *Chem. Phys.* **1987**, *112*, 259.

(5) De Kanter, F. J. J.; den Hollander, J. A.; Huizer, A. H.; Kaptein, R. *Mol. Phys.* **1977**, *34*, 857.

(6) (a) Maeda, K.; Terazima, M.; Azumi, T.; Tanimoto, Y. *J. Phys. Chem.* **1991**, *95*, 197. (b) Maeda, K.; Meng, Q.-X.; Aizawa, T.; Terazima, M.; Azumi, T.; Tanimoto, Y. *J. Phys. Chem.* **1992**, *96*, 4884.

(7) (a) Zimmt, M. B.; Doubleday, C., Jr.; Turro, N. J. *J. Am. Chem. Soc.* **1985**, *107*, 6724. (b) Zimmt, M. B.; Doubleday, C., Jr.; Turro, N. J. *J. Am. Chem. Soc.* **1986**, *108*, 3618. (c) Zimmt, M. B.; Doubleday, C., Jr.; Turro, N. J. *Chem. Phys. Lett.* **1987**, *134*, 549. (d) Wang, J.-F.; Doubleday, C., Jr.; Turro, N. J. *J. Am. Chem. Soc.* **1989**, *111*, 3962. (e) Wang, J.-F.; Rao, V. P.; Doubleday, C., Jr.; Turro, N. J. *J. Phys. Chem.* **1990**, *94*, 1144.

(8) De Kanter, F. J. J.; Kaptein, R. *J. Am. Chem. Soc.* **1982**, *104*, 4759.

(9) Closs, G. L.; Redwine, O. D. *J. Am. Chem. Soc.* **1985**, *107*, 6131.

(10) (a) Tanimoto, Y; Takashima, M.; Hasegawa, K.; Itoh, M. *Chem. Phys. Lett.* **1987**, *137*, 330. (b) Tanimoto, Y; Takashima, M.; Itoh, M. *Bull. Chem. Soc. Jpn.* **1989**, *62*, 3923.

(11) Wang, J.-F.; Doubleday, C., Jr.; Turro, N. J. *J. Phys. Chem.* **1989**, *93*, 4780.

(12) Ball, J. D.; Schulz, G. R.; Wu,T.; Forbes, M. D. E., submitted for publication.

(13) Morozova, O. B.; Yurkovskaya, A. V.; Tsentalovich, Yu.P.; Sagdeev, R. Z.; Wu, T.; Forbes, M. D. E. *J. Phys. Chem. A* **1997**, *101*, 8803.

(14) Saltzmann, M.; Tsentalovich, Yu. P.; Fischer, H. *J. Chem. Soc., Perkin. Trans. 2* **1994**, 2119.

(15) (a) Vollenweider, J.-K.; Fischer, H.; Hennig, J.; Leuschner, R. *Chem. Phys.* **1985**, *97*, 217. (b) Neville, A. G.; Brown, C. E.; Rayner, D. M.; Lusztyk, J; Ingold, K. U. *J. Am. Chem. Soc.* **1991**, *113*, 1869. (c) Tsentalovich, Yu. P.; Fischer, H. *J. Chem. Soc., Perkin Trans. 2* 1994, 729.

(16) (a) Closs, G. L.; and Forbes, M. D. E. *J. Phys. Chem.* **1991**, *95*, 1924. (b) Forbes, M. D. E.; Peterson, J.; Breivogel, C. S. *Rev. Sci. Instrum.* **1991**, *62*, 2662.

(17) Tsentalovich, Yu.P.; Avdievich, N. I.; Forbes, M. D. E., submitted to publication.

(18) Molokov, I. F.; Tsentalovich, Yu.P.; Yurkovskaya, A. V.; Sagdeev, R. Z. *J. Photochem. Photobiol. A: Chem.*, in press.

(19) Bagryanskaya, E. G.; Sagdeev, R. Z. *Prog. React. Kinet.* **1993**, *18*, 63.

(20) (a) Yurkovskaya, A. V.; Tsentalovich, Yu.P.; Lukzen, N. N.; Sagdeev, R. Z. *Res. Chem. Intermed.* **1992**, *17*, 145. (b) Morozova, O. B.; Yurkovskaya, A. V.; Tsentalovich, Yu.P.; Vieth, H.-M: *J. Phys. Chem. A* **1997**, *101*, 399.

(21) Koptuyg, I. V.; Lukzen, N. N.; Bagryanskaya, E. G.; Doktorov, A. B.; Sagdeev, R.Z. *Chem. Phys.* **1992**, *162*, 165.

(22) (a) Closs, G. L.; Forbes, M. D. E.; Norris, J. R. J. *J. Phys. Chem.* **1987**, *91*, 3592. (b) Buckley, C. D.; Hunter, D. A.; Hore, P. J.; McLauchlan, K. A. *Chem. Phys. Lett.* **1987**, *135*, 307.

(23) (a) Gordon, S.; Hart, E. J.; Thomas, J. K. *J. Phys. Chem.* **1964**, *68*, 1262. (b) Simic, M.; Neta, P.; Hayon, E. *J. Phys. Chem.* **1969**, *73*, 3794. (c) Neta, P. *Adv. Phys. Org Chem.* **1976**, *12*, 223. (23) Porter, G.; Dogra, S. R.; Loutfy, R. O.; Sugamuri, S. E.; Yip, R. W. *J. Chem. Soc., Faraday Trans. 1* **1973**, *69*, 1462.

(24) Morozova, O. B.; Tsentalovich, Yu.P.; Yurkovskaya, A. V.; Sagdeev, R. Z., manuscript in preparation.

(25) (a) McLauchlan, K. A.; Stevens, D. G *J. Magn. Reson.* **1985**, *63*, 473. (b) Jent, F.; Paul, H. *Chem. Phys. Lett.* **1989**, *160*, 632. (c) Levstein, P. R.; van Willigen, H. *J. Chem. Phys.* **1991**, *95*, 900.

(26) (a) Avdievich, N. I.; Forbes, M. D. E. *J. Phys. Chem.* **1995**, *99*, 9660. (b) Avdievich, N. I.; Forbes, M. D. E. *J. Phys. Chem.* **1996**, *100*, 1993.

(27) Landolt-Bornstein, New Series, Group II, *Magnetic Properties of Free Radicals*; 1977; Vol. 9b.